

850. Design and numerical analysis of a novel coaxial rotorcraft UAV

Liu Long¹, Ang Haisong², Ge Xun³

College of Aerospace Engineering, Nanjing University of Aeronautics and Astronautics
Mailbox 172, No. 29 Yudao street, Nanjing, Jiangsu, 210016, China

E-mail: ¹liul_1988@163.com, ²ahs@nuaa.edu.com, ³4096366@qq.com

(Received 14 June 2012; accepted 4 September 2012)

Abstract. This paper reports the design of a novel coaxial rotorcraft UAV with canard wing, main wing and tail rotor, which is capable of converting status between contra-rotating case model and fixed wing model. Computational fluid dynamics approach involving momentum source method is adopted to study its aerodynamic characteristics in various states. A validation case is introduced in this paper to verify the reliability and precision of this method. The result proves that the designed coaxial rotorcraft UAV is able to hover, take off and land vertically as well as change between the contra-rotating case model and the fixed wing model. Accordingly, it is able to accomplish various operating statuses and demonstrate good aerodynamic characteristics during the whole flight envelope.

Keywords: coaxial rotorcraft, UAV, momentum source, low Reynolds flow, aerodynamic.

Nomenclature

C_T	=	Thrust Coefficient
C_L	=	Lift coefficient
C_D	=	Drag coefficient
L_D	=	Lift-to-drag ratio

Introduction

Unmanned Aerial Vehicles (UAVs), in particular unmanned helicopters, are drawing more and more attention from researchers all over the world as a result of their capabilities of hovering and Vertical Taking-Off and Landing (VTOL), which meets military demands for effective information-gathering capability in combat situations [1]. Recent work by Yihua Cao has focused on the flight history and development of rotorcrafts [2].

One popular configuration of helicopters is coaxial rotor configuration, which comparing to a single rotor in the conventional design, produces the net thrust and then makes the rotorcraft compact and thus safer during military missions. The traditional rotorcrafts have to balance the angular momentum, usually by the tail rotor, which on the other hand adds the weight and also makes the size larger. Furthermore, a single rotorcraft is inherently directionally less stable and thus less safe to fly at low speeds. The tail rotor sometimes enters the vortex-ring state during sideward flight [3]. While in a coaxial-rotor configuration, the angular momentum is automatically conserved with the counter-rotating coaxial rotors. Useful lift and thrust in the coaxial system are then generated. A coaxial rotorcraft can also be designed with a smaller footprint without the need for separating rotors. However, besides above advantages, the two rotors and their wakes interact with each other, bringing a more complicated flow-field than is found in a single rotor system [4]. Very limited experimental and computational work has been performed on coaxial rotor aerodynamics. Seiko Micro Flying Robot [5] and the Micor [6] are examples of coaxial UAVs, which were developed at the University of Maryland. Also in [6], the performance of coaxial rotor at torque equilibrium was explored. Recent study by Liu performed at different rotor axial spacing to study their mutual interferences on the static performance [7]. For computational studies, there have been various approaches. Slipstream theory was at first introduced to solve the aerodynamics of coaxial rotors, and was further

developed into predicted wake vortex model [8]. Simple (global) momentum theory and the blade element momentum theory (BEMT) were derived by Leishman [9] for a coaxial rotor system in hover. Griffiths and Leishman [10] studied the dual-rotor interactions considering ground effects with the Free Vortex Method (FVM). Vorticity Transport Model (VTM) was used by Kim and Brown [11] to investigate the coaxial rotor system. Xu, et al. investigated the aerodynamics of the coaxial rotor helicopter in hover by solving the unsteady Euler equations based on unstructured dynamic overset grids [12].

In this paper, a new coaxial rotorcraft UAV with unique features has been designed. This paper is organized as follows. In section 1, a new coaxial rotorcraft UAV with several unique features is designed both in CAD model and manufacturing entity. In section 2, CFD simulation method using momentum source model (MSM) is introduced to analyze the aerodynamic characteristics of rotors. A validation case with GIT model using this method is then presented. Section 3 is arranged to analyze the aerodynamic characteristics of the coaxial rotorcraft UAV and examine the interaction of rotors as well as the fuselage and wings. Finally, conclusions are presented for further research in Section 4.

Vehicle design and description

The idea of this UAV came from a combination of rotorcrafts and fixed wing aircrafts considering both features. Boeing X-50 was an early attempt of this Rotor/Wing UAV. Also we consider the advantages of coaxial rotorcrafts instead of the conventional ones. Then we decided to design a novel coaxial rotorcraft UAV. The design features are presented later.

First we designed the main frame comparing with X-50 model and briefly estimated the weight of the whole UAV to determine the lift that the rotors need to provide when hovering. Then the configuration of the coaxial rotors was determined with lift and standard rotating speed as its main design parameters. Finally, we adjusted the position of the coaxial rotors to fit the torques considering the unique features. The main geometry and flight characteristics of the coaxial rotorcraft UAV are presented in Table 1 and Fig. 1. The fuselage and the wings are made of carbon and balsa wood by hand and the swashplate and hub are made by subcontractors. Fig. 2 illustrates the model of the UAV.

Table 1. Rotorcraft UAV parameters

Parameter	Value
Spacing between two rotors	0.09 (m)
Weight of UAV	2.25 (kg)
Cruise speed	18 (m/s)

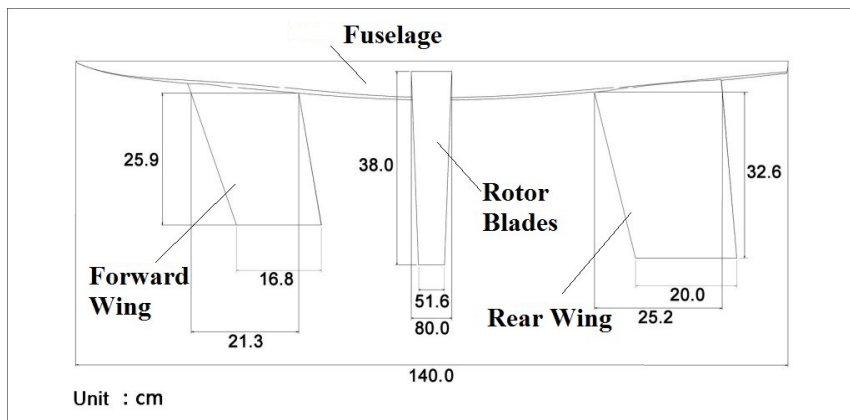


Fig. 1. Main geometry size of the designed UAV

Some significant and unique design features of the UAV are as follows:

- a) Three rotors can be found in this UAV (Fig. 2). A pair of contra-rotating rotors is installed in the middle about 20 mm upper off the fuselage to provide sufficient thrust to allow the UAV hovering and vertical take-off/landing. The tail rotor is installed horizontally at the rear part of the fuselage serving as the propeller to provide needed thrust for maneuver flight.
- b) It is a combination of rotorcraft and fixed-wing UAV, which means when it is cruising, the contra-rotating rotors can also serve as fixed wings to increase the lift and decrease the power consumption. In that case, the tail rotor provides the needed thrust.
- c) The forward wing can also be seen as the canard wing, which also enhances aerodynamic capabilities and provides better maneuver flight performance.
- d) Several conventional control surfaces are submerged in the rotors and wings to improve control authority and flight efficiency.

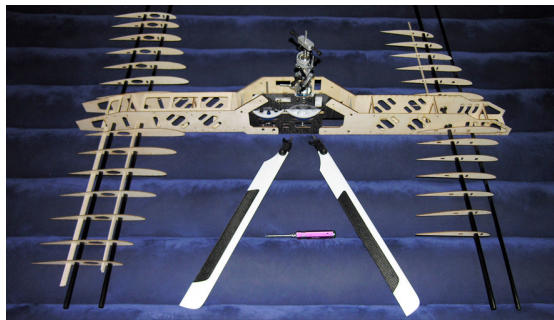


Fig. 2. Preliminary model of the designed UAV

Feasibility and control system description

In this paper, the power and driving system is briefly shown in Fig. 3. With this system, the power of the tail rotor can change smoothly and set the engine in an efficient operating status by sharing the best power ratio with the contra-rotating rotors.

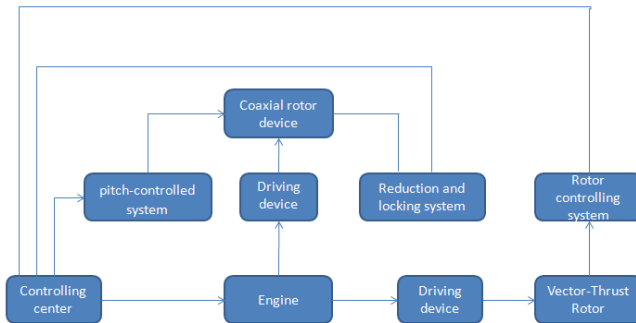


Fig. 3. Power and driving system

CFD simulation

CFD method

Computational Fluid Dynamics (CFD) has been playing an important role in aircraft design because of its efficiency and low-cost characteristic comparing with wind tunnel and PIV experiments. As mentioned in the introduction part, various methods have been used in the 1254

simulation of rotor aerodynamics. Among these methods, FVM and VTM failed in simulating detailed flow features near the blades and blade vortex in the wake [12]. While providing better result, the overset grid method requires high preparation in grid generating process, especially dealing with complicated configurations, and may take much more time. Considering this, the method of momentum source is introduced in this paper.

The actuator disk method was developed by Rajagopalan in which the rotors are treated as actuator disks and the influence of the rotor is modeled as a set of forces applied to the flow field in cells intersecting the rotors [13]. Rotor fuselage interactions were investigated using this method by Zori, et al. [14]. The actuator disk concept consists of modeling the rotor as a permeable volume, with the rotor swept area as its surface, in which a momentum source is applied to capture the pressure change caused by rotating blades. The momentum source items are induced by blade element theory [15] and preconditioned RANS equations [16] are used as the governing equations to simulate low-speed characteristics. In this paper, the momentum source method was examined in FLUENT as UDF with GIT validation case and then applied to the novel rotorcraft UAV.

Validation case

The GIT rotor/airframe interaction model was first used as the validation case for all of the rotor configurations taken in FUN3D and this geometry has been extensively tested [17] in the GIT wind tunnel because of its simplifications as follows:

- a) The blades are defined as nearly rigid blades so the deformation is neglected.
- b) The hub size is the smallest so the hub effect reduces the most.
- c) The fuselage configuration is set to be a simple geometry, which makes the flow effects less difficult to identify.

The GIT configuration consists of a cylindrical fuselage and a two-blade rotor. The parameters of the geometry can be found in [18]. The CFD model and mesh distribution are shown in Fig. 4 and Fig. 5. Here the rotor is replaced by actuator disks. In order to capture the severe change of flow fields around the rotors, meshes are locally refined around the blade tips and rotor hubs shown as concentrated meshes.

The number of surface mesh elements is about 152 thousand and the total number of grid is 6.41 million. We set 12 layers in the boundary layer and the initial height is 0.0008 mm and max Y^+ is then 7. Here we adopted RANS and $k-\varepsilon$ equations as the turbulence model.

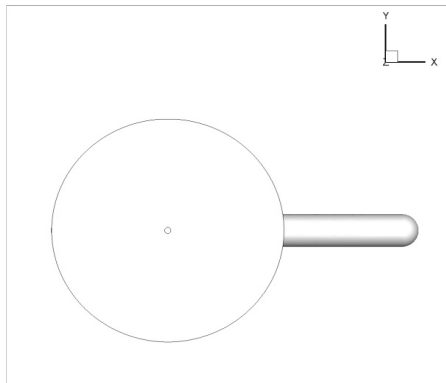


Fig. 4. Main configuration of the GIT model

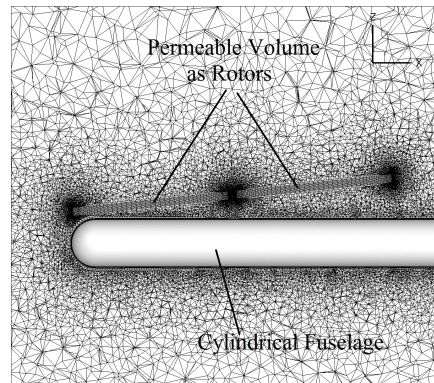


Fig. 5. Mesh of the GIT model

In this case, the rotor speed is 2100 RPM with the tip velocity of 100.5 m/s, which corresponds to a very small free stream velocity of 10.05 m/s to meet the demand of setting

advance ratio of μ to a value of 0.1. The ratio of this value can reduce ground effects and provide sufficient interaction between the rotor and fuselage.

The result in Table 2 and Fig. 6 suggests that the method of momentum source model can provide a relatively reliable numerical result of rotor/airframe interaction and thus feasible in the simulation of rotorcrafts. The experiment data can also be found in [18].

Table 2. Rotor thrust comparison

Thrust Coefficient C_T	Value
Experiment	0.009045
CFD	0.009655

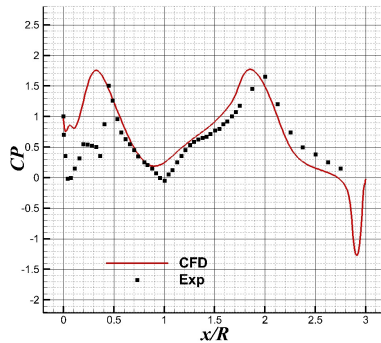


Fig. 6. Pressure coefficient on the upper surface of the fuselage

Rotor blade airfoil

As the contra-rotating rotors serve as fixed wings in some cases, the airfoil of the rotor blade has to be symmetrical bilaterally, which always produces inferior aerodynamic characteristics. Here an unconventional airfoil is designed using CST method [19] considering the symmetrical feature and low-speed characteristic. Fig. 7 and Fig. 8 are the airfoil configuration and Lift characteristic at different angle of attack (AOA).

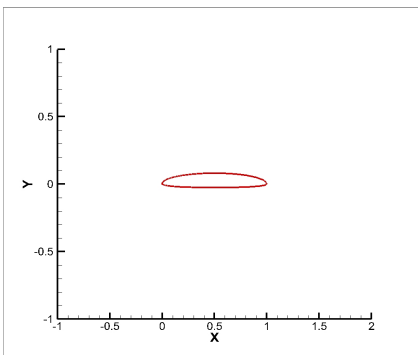


Fig. 7. Geometrical configuration of the airfoil

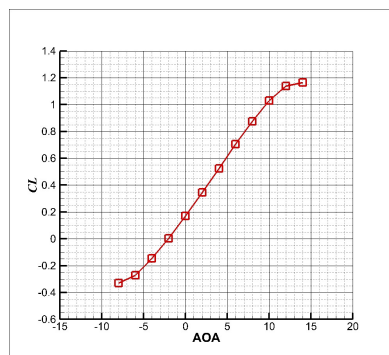


Fig. 8. Lift coefficient at different AOA

Mesh generation

In this paper, two cases are considered with the two upper rotors working as fixed wing or contra-rotating rotors. The former case is defined as fixed wing case in which the two rotors are served as “wings” and only half-model is presented because of its symmetry feature. The latter

case is treated as contra-rotating case, where the rotors are normal rotors and replaced by momentum source cylinder using momentum source method. In both cases the tail rotor, the control surfaces and the winglets are not considered for simplification. Computational grids for both cases are shown in Fig. 9 and Fig. 10.

The total grid size is 3.20 million and 3.5 million for fixed wing case and contra-rotating case respectively. There are 8 layers in the boundary layer and the initial height is 0.1 mm for both cases, which gets 7.3 of the Y^+ .

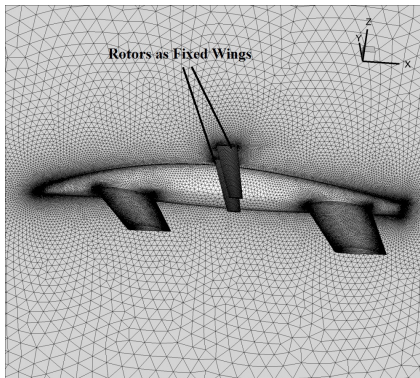


Fig. 9. Mesh for fixed wing case

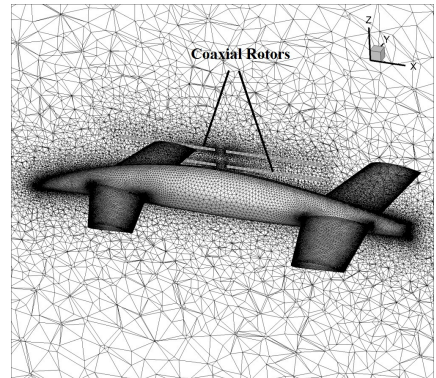


Fig. 10. Mesh for contra-rotating case

Simulation results for fixed wing case

The velocity of the free stream is 18 m/s and the AOA of the free stream ranges from -6 deg to 16 deg. Fig. 11 and Fig. 12 illustrate the aerodynamic characteristics of drag and lift. The result shows that the stall angle is higher than 16 deg and the canard wing improves the aerodynamic performances at high angles, which enables the UAV to accomplish all the missions during the whole flight envelope.

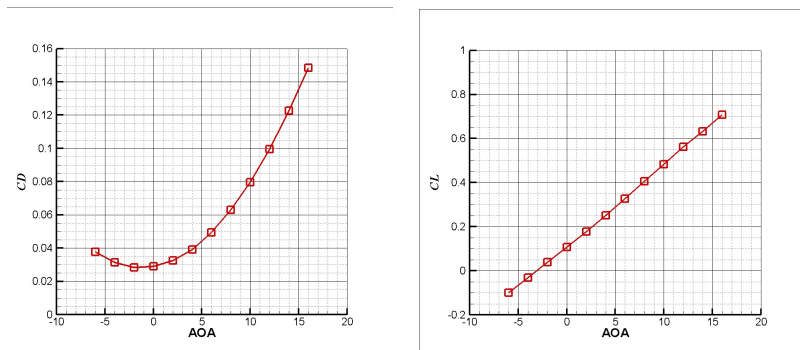


Fig. 11. Drag and Lift coefficient at different angle of attack

According to the lift-to-drag ratio in Fig. 12, which is the best at AOA of 6 deg, the details of lift on each part in this status are presented in Table 3. The rotors demonstrate great advantages in the lift increase as fixed wings.

Comparison between fixed wing case and conventional wing-free case

To illustrate the advantages of the rotors serving as fixed wings, we made a comparison between fixed wing case and the conventional wing-free case. Here we only omit the rotors and

keep the mesh and simulation conditions the same. The results are provided in Fig. 13. We can observe that the lift coefficient is larger in fixed wing case and the lift-to-drag ratio is larger, especially when the angle of attack is higher.

Table 3. Lift contribution

Part	Percentage (%)
Fuselage	10.85
Canard wing	31.56
Main wing	32.76
Rotors	24.38

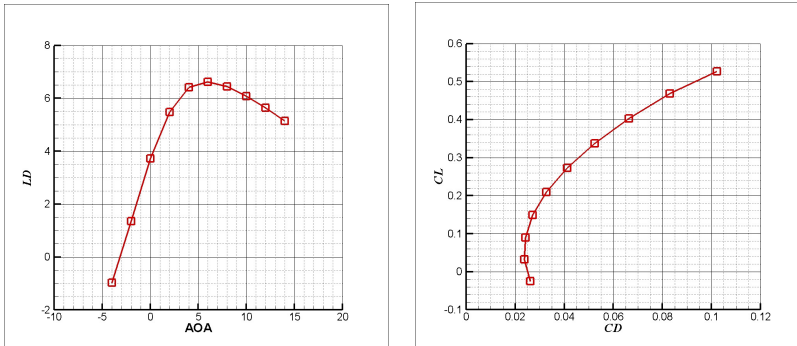


Fig. 12. Lift-to-drag ratio at different angle of attack

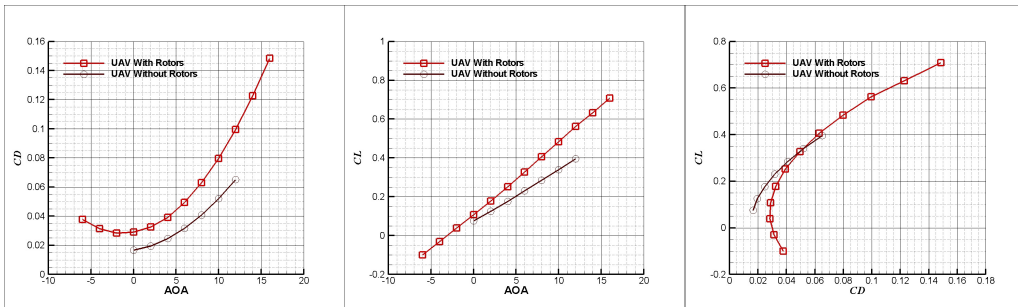


Fig. 13. Comparison of Drag and Lift coefficient and Lift-to-drag ratio at different angle of attack

Simulation results of contra-rotating case

In this case, the effect of the rotors and the interaction of the rotors and the fuselage are fully determined and analyzed. Cases of different rotational speeds and free stream status with corresponding velocity and AOA are simulated in this paper considering various flight missions. Table 4 contains the computational parameters and the simulated thrusts of the rotors. Case 4 simulates the status of UAV in hover by assuming the velocity of the free stream to be relatively small. The stream lines can be observed in Fig. 14. Also the static thrust of rotors is measured using tense sensor equipment in Fig. 15. Considering this, we only have the thrust in Case 4 measured with the equipment in which we assume that this UAV is in hover. The measured thrust is 2420g (about 23.716 N), which is close to the CFD result.

Fig. 16 and Fig. 17 illustrate the pressure and Z velocity distribution for different cases. As can be concluded from Fig. 17(c), the downwash effect caused by contra-rotating rotors has some impacts on the main wing and thus makes the main wing less effective. Also the effect of the rotor declines as the speed of the free stream comes larger.

Table 4. Computational cases and the corresponding thrusts of rotors

	Velocity of free stream (m/s)	AOA of free stream (deg)	Rotational speed (r/min)	Setting angle of blade (deg)	Thrust of the total rotors (N)
Case 1	15	6	1000	0	3.756491
Case 2	10	4	1500	1.5	15.18105
Case 3	5	0	2000	3	29.01091
Case 4	1	90	2000	3	21.36693

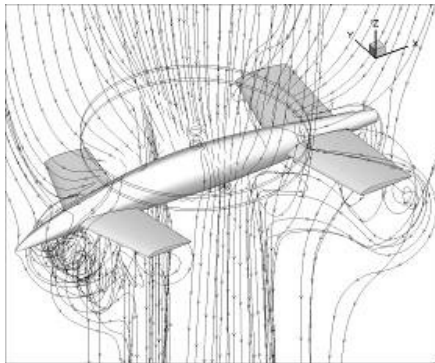
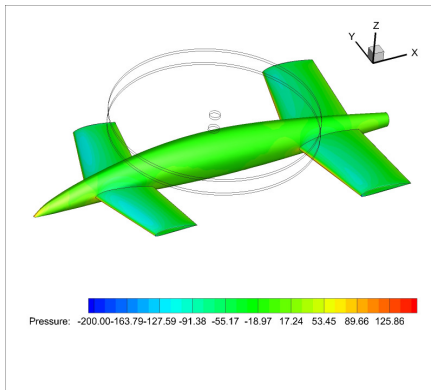


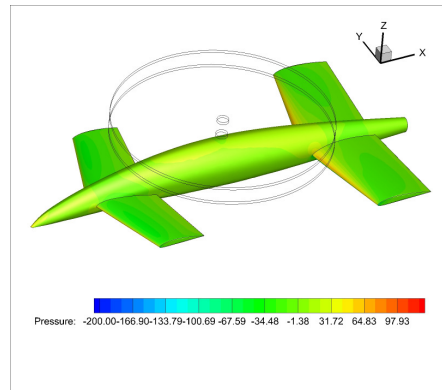
Fig. 14. Stream line distribution in hover



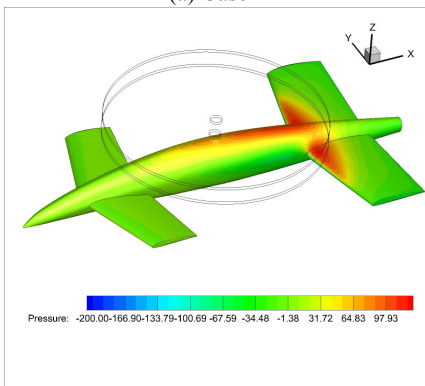
Fig. 15. Thrust measuring equipment



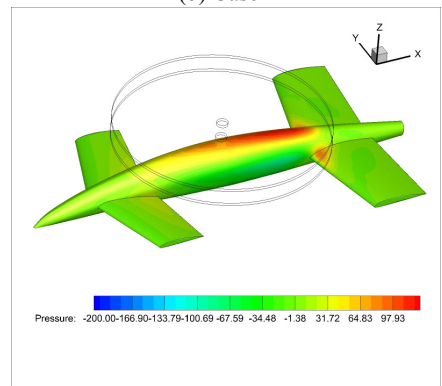
(a) Case 1



(b) Case 2



(c) Case 3



(d) Case 4

Fig. 16. Pressure distribution on the fuselage and wings in each case

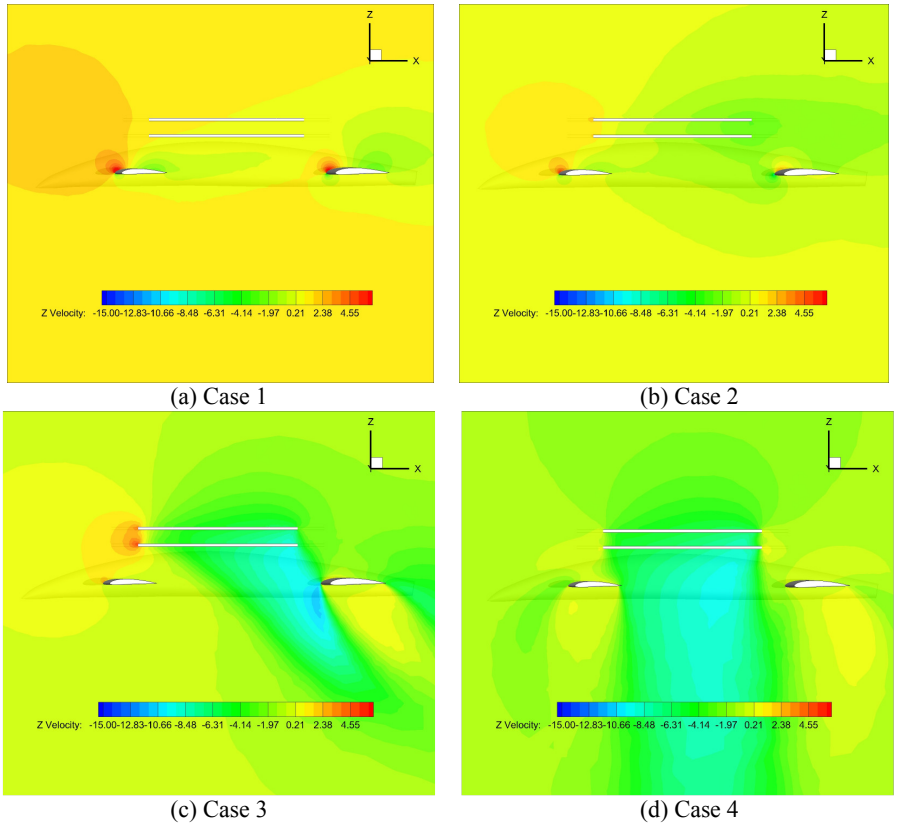


Fig. 17. Z velocity at the plane of $Y = -0.25$ m

Also the pressure distribution on the surface of the rotor volumes can be observed in Fig. 18 and Fig. 19. It is a combination of rotating and free stream effects. The pressure on the upper surfaces is lower than that on the lower surface and the difference values between them produce the thrust. Also from the pressure distribution, it can be concluded that the lower rotor has difference of relatively larger values between two surfaces. This is in accordance with the fact that the upper rotor speeds up the air in the opposite rotating direction comparing to the lower rotor, which corresponds to a larger rotating speed of the lower rotor.

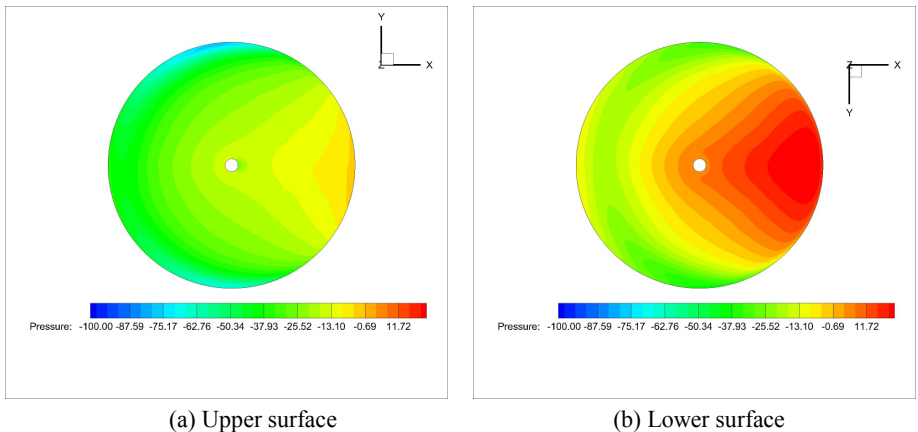
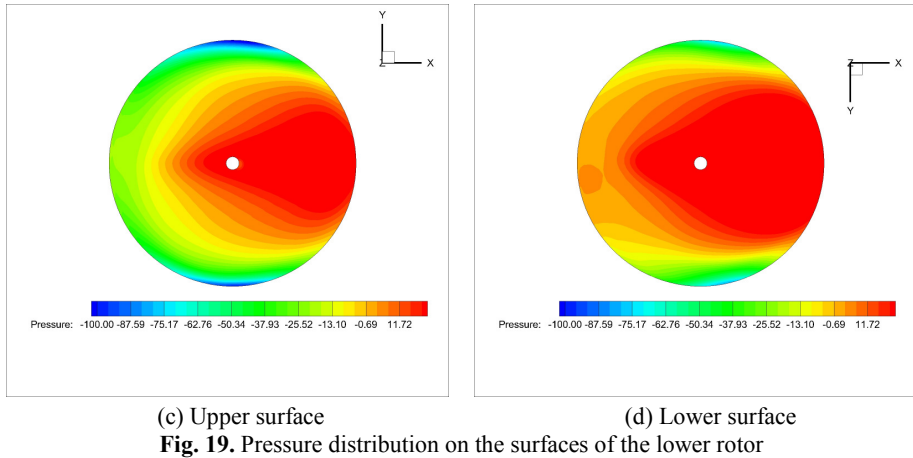


Fig. 18. Pressure distribution on the surfaces of the upper rotor



Conclusion

A novel coaxial rotorcraft UAV was designed and numerically analyzed in this paper. From the result of the validation case, this simulation approach by using momentum source method is proved to be of high precision and reliability. Two cases are considered with different ways of rotor dealings. In fixed wing case, different statuses are simulated with different AOA of the free stream. It is concluded that the stall angle is higher than 16 deg and the canard wing improves the aerodynamic characteristics at high angles. The rotors enhance the capabilities of lift increase as fixed wings as it was expected by the research team. In contra-rotating case, main statuses of different rotational speed of rotors and free stream parameters are simulated considering various missions. Improvement in the configuration about the main wing should be made as a result of the downwash effect caused by contra-rotating rotors. The power and driving system is briefly introduced, which enable the UAV to hover, take off and land vertically, change between contra-rotating mode and fixed wing mode, thus having good aerodynamic characteristics during the whole flight envelope.

Acknowledgements

This research is supported by the Research Fund of Nanjing University of Aeronautics and Astronautics. The first author of this paper would like to thank Professor Xiao Tianhang for his help and suggestions.

References

- [1] **Spanoudakis P., Doitsidis L., Tsurveloudis N.** A market overview of the vertical take-off and landing UAVs. Workshop on Unmanned Aerial Vehicles, 11th Mediterranean Conference on Control and Automation, Rhodes, Greece, 2003.
- [2] **Cao Yihua, Li Dong, Zhang Qiang, Bian Hang** Recent development of rotorcraft configuration. Recent Patents on Engineering, Volume 1, Number 1, February 2007, p. 49-70.
- [3] **Albert B., Mark D., Ron Kisor** The nature of vortex ring state. Journal of the American Helicopter Society, Vol. 56, No. 2, 2011, p. 22001-22014.
- [4] **Vinod K. Lakshminarayan, James D. Baeder** Computational investigation of microscale coaxial-rotor aerodynamics in hover. Journal of Aircraft, Vol. 47, No. 3, May-June 2010.
- [5] Seiko Epson Corporation. Epson Develops World's Smallest Flying Robot, <http://www.epson.co.jp/e/newsroom/news 2003 11 18 2.htm>, November 17, 2003.
- [6] **Bohorquez F.** Rotor Hover Performance and System Design of an Efficient Coaxial Rotary Wing Micro Air Vehicle. Ph. D. Dissertation, Department of Aerospace Engineering, University of

Maryland, College Park, MD, 2007.

- [7] **Liu Z., Albertani R., Moschetta J. M.** Experimental and computational evaluation of small microcoaxial rotor in hover. *Journal of Aircraft*, Vol. 48, No. 1, January-February 2011.
- [8] **Andrew M. J.** Co-axial rotor aerodynamics in hover. *Vertica*, Vol. 5(2), 1981, p. 163-172.
- [9] **Leishman J. G.** *Principles of Helicopter Aerodynamics*. Cambridge University Press, 2002.
- [10] **Griffiths D. A., Leishman J. G.** A study of dual-rotor interference and ground effect using a free-vortex wake model. Proceedings of the 58th Annual Forum of the American Helicopter Society, Montreal, Canada, June 2002.
- [11] **Kim H. W., Brown R. E.** Coaxial rotor performance and wake dynamics in steady and maneuvering flight. Proceedings of the 62nd Annual Forum of the American Helicopter Society, Phoenix, A Z, May 2006.
- [12] **Xu H. Y., Ye Z. Y.** Numerical simulation of interaction of unsteady flows around coaxial rotors. *Journal of Aerospace Power*, 2011, (in Chinese, in press).
- [13] **Rajagopalan R. G., Fanucci J. B.** Finite difference model for vertical axis wind turbines. *Journal of Propulsion and Power*, Vol. 1, No. 6, 1985, p. 432-436.
- [14] **Zori L. A. J., Mathur S. R., Rajagopalan R. G.** Three-dimensional calculations of rotor-airframe interaction in forward flight. Proceedings of the 48th Annual Forum, Washington, DC, American Helicopter Society, June 1992.
- [15] **Johnson W.** *Helicopter Theory*. Princeton University Press, 1980, p. 121-122.
- [16] **Xiao Tianhang, Ang Haisong, Yu Shaozhi** A preconditioned dual time-stepping procedure coupled with matrix-free LU-SGS scheme for unsteady low speed viscous flows with moving objects. *International Journal of Computational Fluid Dynamics*, 2007, Vol. 21, p. 165-173.
- [17] **Liou S. G., Komerath N. M., McMahon H. M.** Measurement of the interaction between a rotor tip vortex and a cylinder. *AIAA Journal*, Vol. 28, Issue 6, p. 975-981.
- [18] **David M. O'Brien** Analysis of Computational Modeling Techniques for Complete Rotorcraft Configurations. Ph. D. Thesis, Georgia Institute of Technology, 2006.
- [19] **Kulfan B. M., Bussoletti J. E.** "Fundamental" Parametric Geometry Representations for Aircraft Component Shape. AIAA-2006-6948, September 2006.